Journal of Global Change Data & Discovery. 2021, 5(2): 120-129
www.geodoi.ac.cn

Development of the Heat Wave Dataset for the Belt and Road Region (1989–2018)

Yin, C.[1,2] Yang, F.[1,3*]

1. Institute of Geographic Sciences and Natural Resources Research, Chinese Academy of Sciences, Beijing 100101, China;
2. College of resources and environment, University of Chinese Academy of Sciences, Beijing 100049, China;
3. Jiangsu Center for Collaborative Innovation in Geographical Information Resource Development and Application, Nanjing 210023, China

Abstract: Heat waves seriously affect the productivity and daily life of human beings. Therefore, they bring great risks and uncertainties for the future development of countries in the Belt and Road region. Accurate and reliable data are an important basis for future research on the spatiotemporal distribution of heat waves and disaster risk in this region. In this study, we use daily monitoring data from 2,833 NOAA meteorological stations as source data and integrated air temperature, humidity and wind speed to calculate apparent temperature based on Humidex. The elevation-correction interpolation method is used to produce the gridded daily apparent temperature dataset from 1989 to 2018. Based on apparent temperature data, we produced an annual heat wave dataset from 1989 to 2018 using the combination of the absolute temperature threshold and relative temperature threshold. The spatial resolution of this dataset is 0.1° in .tif format, with a total size of 233 GB and 99,927 pieces. The dataset consists of two parts: a daily apparent temperature dataset and an annual heat wave dataset. The daily apparent temperature dataset includes three subdatasets: daily mean, minimum and maximum apparent temperature. Each file is named with the corresponding 8-digit date. The annual heat wave dataset includes 5 subdatasets, including two subdatasets based on the combination of climatological relative temperature threshold (CRTT) and absolute temperature threshold (ATT), two subdatasets based on the combination of annual relative temperature threshold (ARTT) and ATT, and one subdataset based on ATT. Each subdataset includes ten attributes, such as the frequency, duration, and intensity of heat waves.

Keywords: heat wave; apparent temperature; the Belt and Road Region; 1989–2018

DOI: https://doi.org/10.3974/geodp.2021.02.02

CSTR: https://cstr.escience.org.cn/CSTR:20146.14.2021.02.02

Dataset Availability Statement:

The dataset supporting this paper was published and is accessible through the *Digital Journal of Global Change Data Repository* at: https://doi.org/10.3974/geodb.2020.09.08.V1 or https://cstr.escience.org.cn/CSTR:20146.11.2020.09.08.V1.

Received: 21-12-2021; **Accepted:** 04-05-2021; **Published:** 25-06-2021

Foundations: The Construction Project of China Knowledge Center for Engineering Sciences and Technology (CKCEST-2020-2-4); Chinese Academy of Sciences (XDA20030302)

***Corresponding Author:** Yang, F., Institute of Geographic Sciences and Natural Resources Research, Chinese Academy of Sciences, yangfei@igsnrr.ac.cn

Data Citation: [1] Yin, C., Yang, F. Development of the heat wave dataset for the Belt and Road Region (1989–2018) [J]. *Journal of Global Change Data & Discovery*, 2021, 5(2): 120–129. https://doi.org/10.3974/geodp.2021.02.02. https://cstr.escience.org.cn/CSTR:20146.14.2021.02.02.

[2] Yin, C., Yang, F. Heat wave dataset for the Belt and Road Region (1989–2018) [J/DB/OL]. *Digital Journal of Global Change Data Repository*, 2020. https://doi.org/10.3974/geodb.2020.09.08.V1. https://cstr.escience.org.cn/STR:20146.11.2020.09.08.V1.

1 Introduction

In recent years, the frequency of heat wave events around the world has shown an increasing trend, causing serious casualties and property losses. In 2003, a severe heat wave occurred in Western Europe, and the temperature reached the highest level since 1500[1], resulting in approximately 70,000 deaths[2] and a decrease of more than 23 million tons in grain production compared with the same period in the previous year[3]. In 2010, a heat wave in Russia claimed approximately 54,000 lives[4,5]. In 2009, a heat wave in southeastern Australia killed 374 people and triggered devastating forest fires. In 2015, India was hit by an intense heat wave, resulting in more than 2,500 deaths across the country. Heat waves refer to high-temperature weather that lasts for several days. Global warming will continue to enhance the frequency, duration and intensity of heat waves[8]. Coupled climate model results show that in the second half of the 21st century, heat waves will become more frequent, longer lasting and more intense[9,10].

The Belt and Road Region covers 3 continents and more than 66 countries and regions, and approximately 4.4 billion people[11], who are seriously affected by meteorological disasters. From 1995 to 2015, among the 10 countries most severely affected by meteorological disasters in the world, countries in the Belt and Road Region accounted for 7[12]. In addition, numerous countries along the Belt and Road are developing countries with limited ability to withstand natural disasters, and it is one of the regions with the most frequent and severe losses from natural disasters in the world[13]. Heat wave disasters have brought great risks and uncertainties to the advancement of the Belt and Road Initiative. Further study of the spatiotemporal distribution of heat waves in the region can provide information and decision-making support for the government, residents, enterprises, and tourists and can play a guiding role in the government's disaster prevention and mitigation and development planning, residents' lives, enterprise investment and tourist travel planning. In this study, based on meteorological observation data, we produced daily apparent temperature and annual heat wave datasets.

2 Metadata of the Dataset

The metadata of the Heat wave dataset for the Belt and Road Region (1989–2018) is summarized in Table 1. It includes the dataset full name, short name, authors, year of the dataset, temporal resolution, spatial resolution, data format, data size, data files, data publisher, and data sharing policy, etc.

3 Data Development Method

In this study, meteorological observation data are used as the source data to calculate apparent temperature by integrating air temperature, humidity, and wind speed. The interpolation method based on elevation correction is used to produce the daily apparent temperature dataset. Then, the combined threshold method is used to produce the annual heat wave dataset.

3.1 Algorithm Principle

3.1.1 Elevation-correction Interpolation Method

In this study, we use the monitoring data of 2,833 NOAA meteorological stations as the

source data[1]. Because of the discrete distribution of meteorological stations in the study area, interpolation is needed. In addition, due to the large study area, the vertical variation in temperature must be considered; therefore, we adopt the interpolation method based on elevation correction[16–19].

Table 1 Metadata summary of the Heat wave dataset for the Belt and Road Region (1989–2018)

Item	Description
Dataset full name	Heat wave dataset for the Belt and Road Region (1989–2018)
Dataset short name	HeatWave_Belt&Road_1989-2018
Authors	Yin, C. ABA-9865-2020, Institute of Geographic Sciences and Natural Resources Research，Chinese Academy of Sciences, yinc.18s@igsnrr.ac.cn Yang, F., Institute of Geographic Sciences and Natural Resources Research，Chinese Academy of Sciences, yangfei@igsnrr.ac.cn
Geographical region	the Belt and Road Region　Year　1989–2018
Temporal resolution	Year　Spatial resolution　0.1°
Data format	.tif　Data size　233 GB
Data files	Daily apparent temperature dataset and annual heat wave dataset (frequency, duration and intensity)
Foundation	The Construction Project of China Knowledge Center for Engineering Sciences and Technology (CKCEST-2020-2-4); Chinese Academy of Sciences (XDA20030302)
Computing environment	Python
Data publisher	Global Change Research Data Publishing & Repository, http://www.geodoi.ac.cn
Address	No. 11A, Datun Road, Chaoyang District, Beijing 100101, China
Data sharing policy	***Data*** from the Global Change Research Data Publishing & Repository includes metadata, datasets (in the *Digital Journal of Global Change Data Repository*), and publications (in the *Journal of Global Change Data & Discovery*). ***Data*** sharing policy includes: (1) ***Data*** are openly available and can be free downloaded via the Internet; (2) End users are encouraged to use ***Data*** subject to citation; (3) Users, who are by definition also value-added service providers, are welcome to redistribute ***Data*** subject to written permission from the GCdataPR Editorial Office and the issuance of a ***Data*** redistribution license; and (4) If ***Data*** are used to compile new datasets, the 'ten per cent principal' should be followed such that ***Data*** records utilized should not surpass 10% of the new dataset contents, while sources should be clearly noted in suitable places in the new dataset[15]
Communication and searchable system	DOI, CSTR, Crossref, DCI, CSCD, CNKI, SciEngine, WDS/ISC, GEOSS

According to this method, the temperature decreases linearly with increasing altitude (0.006,5 °C/m). The method consists of three steps. First, the observed temperature is transformed to temperature at zero altitude, that is, 0.006,5 °C/m on the basis of the observed temperature plus the temperature decrease due to above zero altitude. Second, the kriging method is used for interpolation based on the corrected temperature. Finally, the interpolated temperature is corrected to the real altitude, that is, on the basis of the interpolated temperature, 0.006,5 °C /m minus the temperature decrease due to elevation above zero.

3.1.2 Apparent Temperature

The adverse effects of heat waves on human health have been widely studied and reported[20–22]. The human body's perception of cold and heat to the external environment is comprehensively affected by air temperature, wind speed, humidity, solar radiation and other

[1] NOAA. https://www.ncei.noaa.gov/data/global-summary-of-the-day/access/.

factors[23,24]. Based on the availability of data and calculation methods, we focus on air temperature, humidity, and wind speed. Obviously, apparent temperature can more accurately reflect the human body's cold and hot feelings than air temperature. The Humidex index is simple to calculate and highly interpretable[25]. It has been increasingly and widely used in the evaluation of human comfort[23,26]. The index considers air temperature and dew point temperature and is calculated as follows:

$$AT = T_a + 0.5555 \times \left(6.11 \times e^{5417.753 \times \left(\frac{1}{273.16} - \frac{1}{T_d + 273.15} \right)} - 10 \right) \# \quad (1)$$

where AT is the apparent temperature (°C), T_a is the air temperature (°C), and T_d is the dew point temperature (°C).

3.1.3 Combined Heat Wave Threshold

Different regions have different standards for defining heat waves[27–29]. For example, the World Meteorological Organization (WMO) defines the weather process in which the daily maximum temperature exceeds 32 °C and lasts for more than 3 days as a heat wave[22]. Most of China adopts 35 °C as the high-temperature threshold. Therefore, it is unreasonable to use the same heat wave threshold for the entire region[30]. In the combined heat wave threshold (CHWT) method, we use the combination of the relative temperature threshold (RTT) and absolute temperature threshold (ATT) to define heat waves.

For the climatological relative temperature threshold (CRTT): when the temperature of a certain location is higher than the long-term historical temperature, the possibility of heat waves increases. Therefore, for each date, we rank the apparent temperature of each grid from 1989 to 2018, select the temperature corresponding to different percentiles as the RTT to judge heat waves, and define it as the CRTT. CHWT allows setting different percentile thresholds to adapt to different heat wave standards.

For the annual relative temperature threshold (ARTT): when the temperature of a certain day is at a high level in the daily temperature series of that year, it also reflects the possibility of heat waves. Therefore, for each year, we rank the daily apparent temperature of each grid and select different percentile thresholds to define RTT, namely, ARTT.

For the absolute temperature threshold (ATT): when the temperature reaches RTT, heat waves do not necessarily occur (such as in winter). Therefore, we also set an absolute temperature threshold to avoid this situation. In this study, we use different combinations of RTT and ATT to define a high-temperature threshold. The weather process that reaches the high-temperature threshold and duration threshold (DT) is called a heat wave.

3.2 Technical Route

The main process of dataset development is as follows. First, the daily monitoring data from NOAA meteorological stations is downloaded, including the observation records of temperature, wind speed, humidity and other variables, and the missing values and outliers are processed. Second, the monitoring data from meteorological stations are interpolated into grid data by using the elevation-correction interpolation method. Then, the daily apparent temperature grid data are calculated based on Humidex. Finally, the combined heat wave threshold method is used to produce an annual heat wave dataset in the Belt and Road region, which mainly includes the frequency, duration, and intensity of heat waves. The technical route is shown in Figure 1.

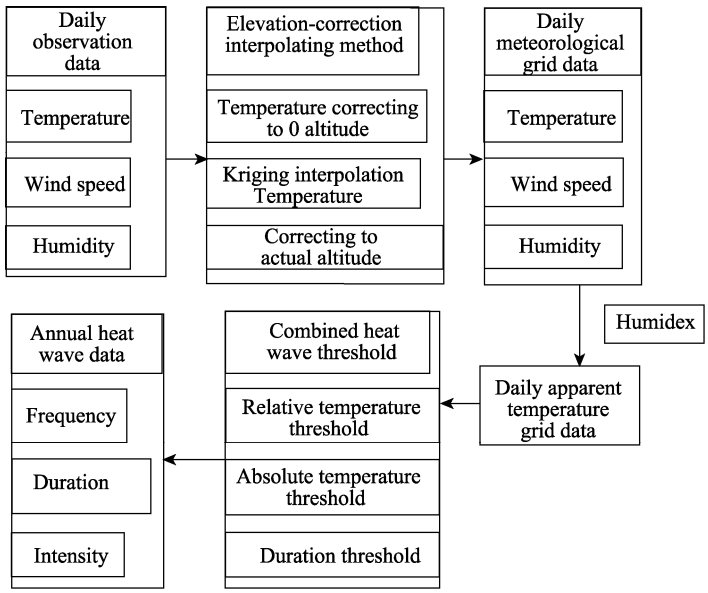

Figure 1 Technical route of the dataset development

4 Data Results and Validation

4.1 Dataset Composition

The 1989–2018 heat wave dataset of the Belt and Road region includes two parts: a daily apparent temperature dataset and an annual heat wave dataset. The daily apparent temperature dataset includes three sub datasets of daily mean, minimum and maximum apparent temperature file is named with the corresponding 8-digit date. The annual heat wave dataset includes five sub-datasets, two of them are based on the combination of CRTT and ATT, two based on the combination of ARTT and ATT, and one based on ATT. Each sub-dataset includes 10 attribute items, such as the frequency, duration, and intensity of heat waves.

4.2 Data Results

Figure 2 shows the mean apparent temperature of 6 days in the Belt and Road region in 2018. On January 1 (Figure 2a), the apparent temperature in Southeast Asia, South Asia and the Arabian Peninsula reached above 20 °C, and the extreme apparent temperature in Indonesia reached even above 40 °C. In eastern China and most regions of Europe, the apparent temperature was approximately 0 °C; in the hinterland of the Eurasian continent, the apparent temperature was between –10 °C and –20 °C; and in the Russian Far East, the extreme apparent temperature was below –40 °C. On March 1 (Figure 2b), with the northward shift of direct solar radiation, the regional apparent temperature near the Tropic of Cancer continued to rise, while the low temperature area in the northern Eurasian continent expanded. Extreme cold temperatures in eastern Siberia moved westward, and the apparent temperature in Europe decreased to approximately –10 °C. On May 1 (Figure 2c), the high-temperature region expanded northward, and the apparent temperature in the region south of 30° N generally reached more than 30 °C. The apparent temperature in most regions in the middle of the Eurasian continent was approximately 0 °C, and the extremely low temperature rose to –25 °C. On July 1 (Figure 2d), the area of the high-temperature area

reached the maximum value for the six dates. The extreme maximum temperature appeared on the India-Pakistan border, reaching above 40 °C, and the apparent temperature in the Eurasian hinterland reached approximately 20 °C. On September 1 (Figure 2e), the overall apparent temperature began to decrease, and the high-temperature area shrank southward, but extreme apparent temperatures above 50 °C appeared in India and Pakistan. On November 1 (Figure 2f), the apparent temperature continued to show a decreasing trend, and the high-temperature area was limited to within the tropics.

Table 1 Dataset composition and description

Folder name	Data content	Nomenclature	Data introduction	Data format	Data record	Data volume
HTMEAN_yyyy_1 (2)	Daily mean apparent temperature of the first (second) half of yyyy	yyyymmdd	Mean apparent temperature	.tif	10,975	74.8 GB
HTMIN_yyyy_1 (2)	Daily minimum apparent temperature of the first (second) half of yyyy	yyyymmdd	Minimum apparent temperature	.tif	10,975	74.7 GB
HTMAX_yyyy_1 (2)	Daily maximum apparent temperature of the first (second) half of yyyy	yyyymmdd	Maximum apparent temperature	.tif	10,975	74.7 GB
HW_HTMEAN_CRTT_90_29_3	HTMEAN, CRTT=90, ATT=29, DT=3	yyyy_freq yyyy_dura yyyy_dmean yyyy_dmin yyyy_dmax yyyy_tmean yyyy_tmin yyyy_tmax yyyy_start yyyy_end	Frequency Total duration Mean duration Maximum duration Minimum duration Mean apparent temperature Minimum apparent temperature Maximum apparent temperature Start date of the first heat wave End date of the last heat wave	.tif	150	9.25 GB
HW_HTMEAN_CRTT_95_29_3	HTMEAN, CRTT=95, ATT=29, DT=3					
HW_HTMEAN_ARTT_80_29_3	HTMEAN, ARTT=80, ATT=29, DT=3					
HW_HTMEAN_ARTT_85_29_3	HTMEAN, ARTT=85, ATT=29, DT=3					
HW_HTMEAN_ATT_29_3	HTMEAN, ATT=29, DT=3					

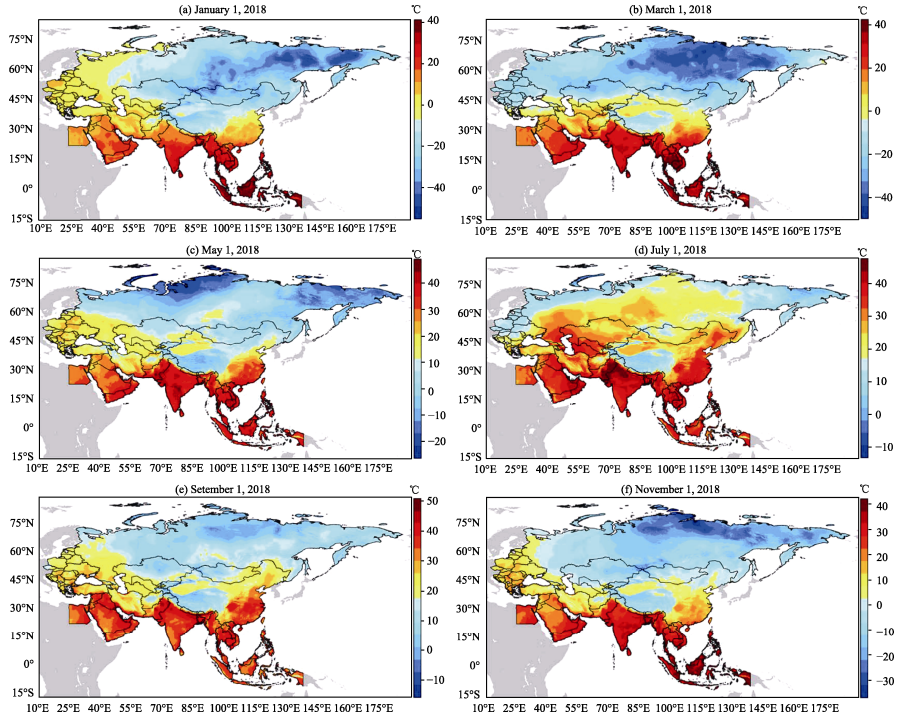

Figure 2 Daily apparent temperature

Based on ARTT=80, ATT=29, and DT=3, Figure 3 shows the main attributes of heat waves in the Belt and Road region in 2018. In 2018, the southeastern coast of China, northern Southeast Asia, northern South Asia, and parts of the Arabian Peninsula had the highest frequency of heat waves, reaching more than eight times. Except for the Qinghai-Tibet Plateau, the frequency of heat waves in the region south of 45°N was generally 4–6 times, while no heat waves were detected in other regions (Figure 3a).

Eastern China, South Asia and West Asia had the longest heat wave duration, lasting more than 40 days, and the longest single heat wave duration in these regions was also longer (Figure 3b, c). The extreme apparent temperature in eastern China reached more than 40 °C, while in South Asia, it reached more than 50 °C (Figure 3d). According to Figure 3e and Figure 3f, the first heat wave started earlier in the southern area of the Belt and Road region, while the last heat wave ended later, while the opposite was true in the north. Specifically, the start date of the first heat wave in southern China, South Asia and the Arabian Peninsula was approximately the 120th day, while the end date of the last heat wave was approximately the 250th day.

4.3 Verification of Data Results

Based on ARTT=80, ATT=29, and DT=3, Figure 4 shows heat wave events in western Russia in 2010 to compare the results of this study with the work of Raei *et al*.[31]. According to the results of this study, a total of 3–5 heat waves were detected in western Russia in 2010 (Figure 4a1), and the total duration of heat waves was 25–40 days, with the longest duration lasting 20–30 days. The total duration of the heat wave near Moscow lasted 40 days, among which the longest heat wave lasted for 30 days (Figure 4b1, 4c1).

The extreme apparent temperature in western Russia was 34–38 °C (Figure 4d1). The first heat wave occurred from 170–200 days, and the last heat wave ended from 220–240 days (Figure 4e1, 4f1). Raei *et al*. established the probability distribution function of daily temperature in different time windows and defined heat waves by the temperature corresponding to different percentile thresholds. Based on a 21-day time window, the 90th percentile, and a 3-day duration. Figure 3 shows the results calculated by Raei *et al*. Compared with the results of this study, the frequency and total duration of heat waves are close to each other, but the spatial distribution is very different, and the high value area is relatively discrete (Figure 4a2, 4b2).

The heat wave with the longest duration was detected near Moscow, lasting 10–12 days (Figure 4c2, 4d2). The spatial distribution of extreme apparent temperature, the start date of the first heat wave and the end date of the last heat wave are difficult to explain. First, it is unreasonable for the temperature to be lower than 0 °C in the area where heat waves occur. Second, for western Russia, it is not practical to detect a large area of heat waves after 300 days (Figure 4e2, 5f2). In general, the results of this study are basically consistent with existing studies but with better interpretability and higher spatial resolution.

5 Discussion and Conclusions

(1) In this study, a dataset of heat waves in the Belt and Road region from 1989 to 2018 was developed pared with air temperature, using apparent temperature can more accurately reflect the real feeling of the human body toward the external environment. Therefore, the heat wave dataset produced based on apparent temperature is more accurate and reliable.

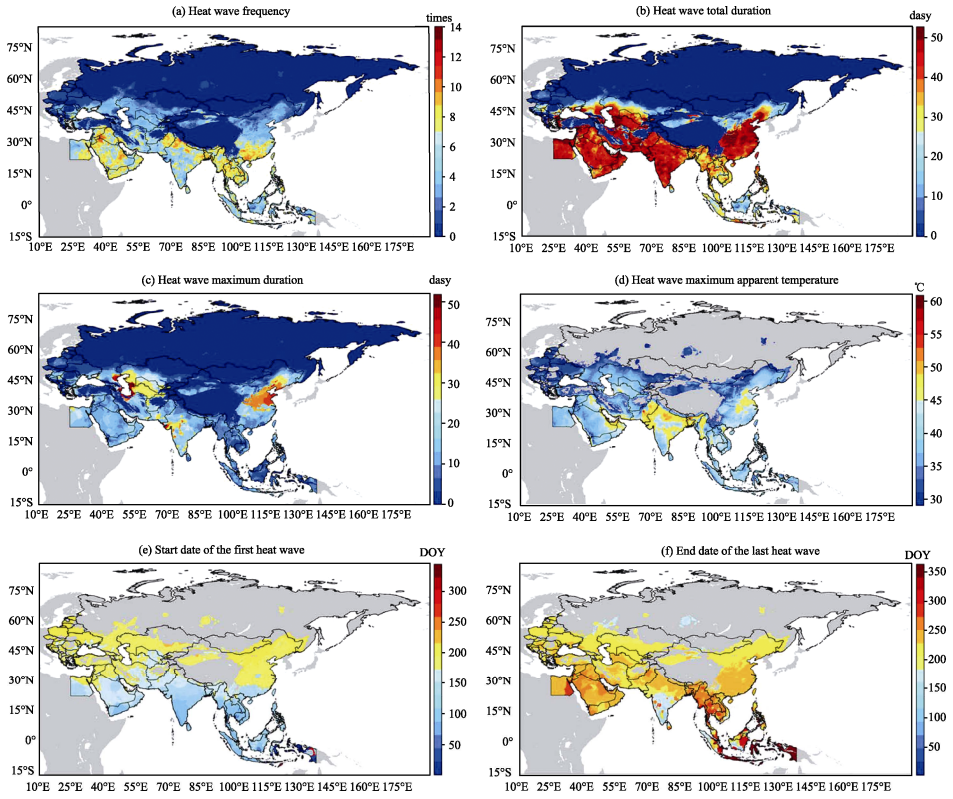

Figure 3 Heat waves in 2018 (ARTT=80, ATT=29, DT=3)

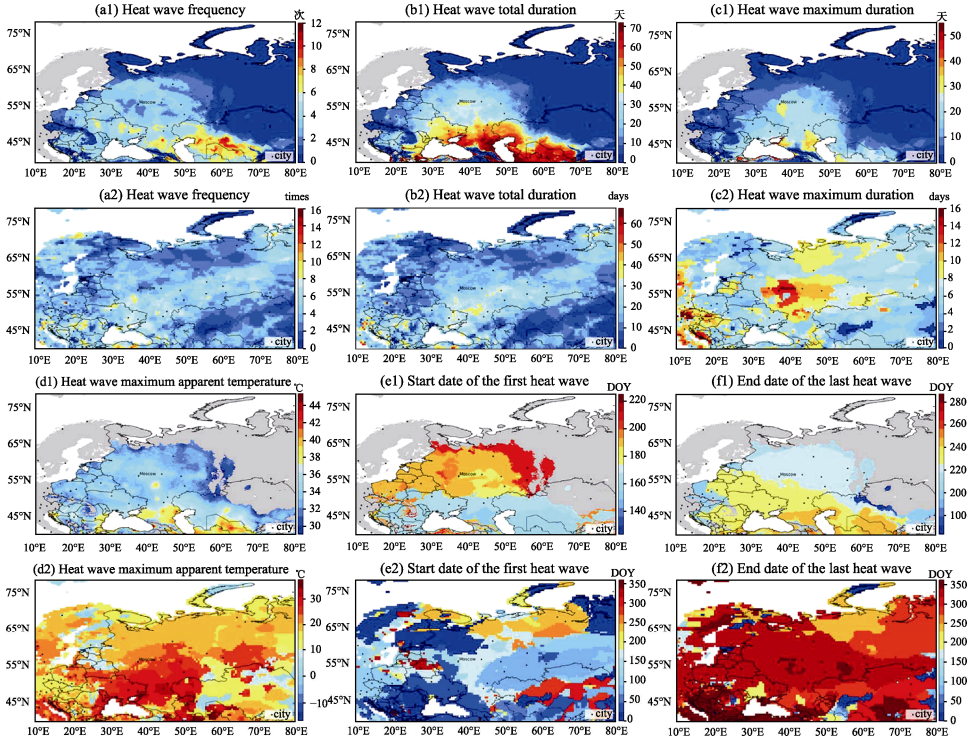

Figure 4 Comparison with the work of Raei *et al.* (the heat wave event in western Russia in 2010)

(2) In this study, the combination of the absolute temperature threshold and relative temperature threshold was adopted to calculate heat waves, making the heat wave threshold more in line with the actual situation of different periods in different places. In addition, the different combinations of each threshold can be adjusted to meet different use needs. (3) The dataset developed in this study has higher spatial resolution and can display more details.

By comparing typical heat wave events with other research results, the results presented in this dataset are more reasonable, more detailed, and more scientific. This dataset can provide data support for research related to heat waves.

Author Contributions

Yang, F. designed the overall dataset; Yin, C. collected and processed heat wave datasets in the One Belt and One Road region from 1989 to 2018 based on apparent temperature. Yin, C. designed the model and algorithm. Yin, C. performed data verification; Yin, C. wrote data papers and so on.

Conflicts of Interest

The authors declare no conflicts of interest.

References

[1] Luterbacher, J., Dietrich, D., Xoplaki, E., *et al*. European seasonal and annual temperature variability, trends, and extremes since 1500 [J]. *Science*, 2004, 303(5663): 1499–1503.

[2] Coumou, D., Rahmstorf, S. A decade of weather extremes [J]. *Nature climate change*, 2012, 2(7): 491.

[3] De Bono, A., Giuliani, G., Kluser, S., *et al*. Impacts of summer 2003 heat wave in Europe [J]. *Environment Alert Bulletin*, 2004, 35(1/2): 19–24.

[4] Gutterman, S. Heat, smoke sent Russia deaths soaring in 2010: govt [N]. Healthcare & Pharma, 2010.

[5] Mcmichael, A. J., Lindgren, E. Climate change: present and future risks to health, and necessary responses [J]. *Journal of internal medicine*, 2011, 270(5): 401–413.

[6] Carnie, J. January 2009 Heatwave in Victoria: an assessment of health impacts [R]. Victorian Government Department of Human Services, Melbourne, 2009.

[7] Mazdiyasni, O., Aghakouchak, A., Davis, S. J., *et al*. Increasing probability of mortality during Indian heat waves [J]. *Science Advances*, 2017, 3: e1700066.

[8] Yan, H. M., Chen, W. N., Yang, F. X., *et al*. Spatial and temporal patterns of extreme climate events in Inner Mongolia during the past 50 years [J]. *Geographical Research*, 2014, 33(01): 13–22.

[9] Meehl, G. A., Tebaldi, C. More intense, more frequent, and longer lasting heat waves in the 21st century [J]. *Science*, 2004, 305(5686): 994–997.

[10] Perkins-Kirkpatrick, S., Alexander, L., Nairn, J. Increasing frequency, intensity and duration of observed global heatwaves and warm spells [J]. *Geophysical Research Letters*, 2012, 39(20): L20714.

[11] Peng, C., Regmi, A. D., Qiang, Z., *et al*. Natural Hazards and Disaster Risk in One Belt One Road Corridors [C]. Proceedings of the Workshop on World Landslide Forum, 2017.

[12] Cui, P., Su, F. H. Application of domestic high resolution satellite in natural disaster risk management of the Belt and Road Initiative [J]. *Satellite Application*, 2016, 10: 8–11.

[13] Mao, X. Z., Liu, J. H., Li, T. S., *et al*. Spatial and temporal distribution characteristics of natural disasters in countries along the Belt and Road [J]. *Journal of Natural Disasters*, 2018, 27(1): 1–8.

[14] Yin, C., Yang, F. Dataset of high temperature and heat wave in the Belt and Road Region (1989–2018) [J /DB/OL]. *Digital Journal of Global Change Data Repository*, 2020. https://doi.org/10.3974/10.3974/geodb.2020.09.08.V1. https://cstr.escience.org.cn/STR:20146.11.2020.09.08.V1.

[15] GCdataPR Editorial Office. GCdataPR data sharing policy [OL]. https://doi.org/10.3974/dp.policy.2014.05 (Updated 2017).

[16] Li, M., Wang, X. L., Ding, Y. Y. Comparison of several daily temperature interpolation methods [J]. *Anhui Agricultural Science*, 2014, (25): 8670–4.

[17] Chen, D. H., Chen, Z., Wang, S. Y., *et al*. Study on spatial interpolation of the average temperature in the Yili River Valley based on DEM [J]. *Spectroscopy & Spectral Analysis*, 2011, 31(7): 1925–1929.

[18] Zhao, J., Fei, L., Fu, H., *et al.* A DEM-based partition adjustment for the interpolation of annual cumulative temperature in China [C]. Proceedings of SPIE—the International Society for Optical Engineering, 2007.

[19] Pan, Y., He, C., Zhang, Q., *et al*. Smart distance searching and DEM-informed interpolation of surface air temperature of climatology in China [C]. Proceedings of the IGARSS 2004 2004 IEEE International Geoscience and Remote Sensing Symposium, 2004.

[20] Khanjani, N., Bahrampour, A. Temperature and cardiovascular and respiratory mortality in desert climate: a case study of Kerman, Iran [J]. *Iranian Journal of Environmental Health Science & Engineering*, 2013, 10(1): 11.

[21] Lowe, D., Ebi, K. L., Forsberg, B. Heatwave early warning systems and adaptation advice to reduce human health consequences of heatwaves [J]. *International Journal of Environmental Research and Public Health*, 2011, 8(12): 4623–48.

[22] Wang, Y., Nordio, F., Nairn, J., *et al*. Accounting for adaptation and intensity in projecting heat wave-related mortality [J]. *Environmental Research*, 2018, 161: 464–471.

[23] Li, N., Xu, Y. M., He, M., *et al*. Retrieval of apparent temperature in Beijing based on remote sensing [J]. *Journal of Ecology and Environment*, 2018, 27(6): 1113–1121.

[24] Hodder, S. G., Parsons, K. The effects of solar radiation on thermal comfort [J]. *International Journal of Biometeorology*, 2007, 51(3): 233–50.

[25] Masterson, J., Richardson, F. A. Humidex: a method of quantifying human discomfort due to excessive heat and humidity, Environment Canada [Z]. Environment Canada, Atmospheric Environment Service, Ontario, Canada, 1979.

[26] Francesca Romana, D. A. A., Boris Igor, P., Giuseppe, R. Thermal environment assessment reliability using temperature—humidity indices [J]. *Industrial Health*, 2011, 49(1): 95–106.

[27] Bobb, J. F., Dominici, F., Peng, R. D. A Bayesian model averaging approach for estimating the relative risk of mortality associated with heat waves in 105 U. S. cities [J]. *Biometrics*, 2011, 67(4): 1605–1616.

[28] Roetzel, A., Tsangrassoulis, A., Dietrich, U., *et al*. A review of occupant control on natural ventilation [J]. *Renewable & Sustainable Energy Reviews*, 2010, 14(3): 1001–1013.

[29] Zuo, J., Pullen, S., Palmer, J., *et al*. Impacts of heat waves and corresponding measures: a review [J]. *Journal of Cleaner Production*, 2015, 92: 1–12.

[30] Chen, Y., Li, Y. An Inter-comparison of three heat wave types in China during 1961–2010: observed basic features and linear trends [J]. *Scientific Reports*, 2017, 7(1): 45619.

[31] Raei, E., Nikoo, M. R., Aghakouchak, A., *et al.* Data descriptor: GHWR, a multi-method global heatwave and warm-spell record and toolbox [J]. *Scientific Data*, 2018, 5(1): 180206.